# Towards energy efficiency of interdependent urban networks


## Giuseppe Alonge

ENEA Piazza,
Ignazio Florio,
24 – 90141 Palermo, Italy
Email: giuseppe.alonge@enea.it

## Ester Ciancamerla

ENEA via Anguillarese,
301 – 00123, Rome, Italy
Email: ester.ciancamerla@enea.it

## Alberto Mastrilli

ENEA Piazza,
Ignazio Florio,
24 – 90141 Palermo, Italy
Email: alberto.mastrilli@enea.it

## Michele Minichino* and Angelo Nicotra

ENEA via Anguillarese,
301 – 00123, Rome, Italy
Email: michele.minichino@enea.it
Email: angelo.nicotra@enea.it
*Corresponding author

## Marco Ranno

Cogip via Trinacria,
15 – 95030 Catania, Italy
Email: marco.ranno@cogip.it

## Maurizio Reali

ENEA via Anguillarese,
301 – 00123, Rome, Italy
Email: maurizo.reali@enea.it

## Pasquale Regina

ENEA via Roberto da Bari,
119 – 70122 Bari, Italy
Email: pasquale.regina@enea.it


**Abstract:** Modernised urban networks will constitute the backbone of smart cities. Modernisation of urban networks is far from being realised and an extensive use of comprehension, and of models at adequate level of granularity, is needed. The paper proposes a cross-domain methodology to represent and evaluate energy efficiency of interdependent urban smart grid, gas and water networks. Models use domain simulators to faithfully represent each physical network, and transversal simulators to represent the three interdependent physical networks, their interdependencies and to compute energy efficiency indicators. Models built by domain simulators are also used to validate models built by transversal simulators. An actual smart grid connected to photovoltaic plants of different power and location is modelled and its efficiency indicators are analysed and discussed. The grid model will be then interconnected with basic gas and water network models to investigate the impact of their interdependencies on energy efficiency indicators.

**Keywords:** smart city; smart grid; gas network; water network; supervisory control and data acquisition; SCADA; energy efficiency; interdependency; model.

**Reference** to this paper should be made as follows: Alonge, G., Ciancamerla, E., Mastrilli, A., Minichino, M., Nicotra, A., Ranno, M., Reali, M. and Regina, P. (2016) 'Towards energy efficiency of interdependent urban networks', *Int. J. Simulation and Process Modelling*, Vol. 11, No. 6, pp.529–546.

**Biographical notes:** Giuseppe Alonge received his Electronic Engineering degree from Palermo University, Italy. Since 2000, he has been working as a researcher at ENEA. He has a long experience in Simulink/MATLAB. He has been developing models to represent interdependent urban networks with the aim of optimising energy efficiency.

Ester Ciancamerla received his Nuclear Engineering degree from University of Rome in 1978. Her current research interest is on modelling methods and tools for dependability/survivability evaluation of networked systems.

Alberto Mastrilli graduated from the University of Palermo in Geographic Information System. Currently, he works on measurement of climatic parameters and atmospheric constituents, and with models of urban water network, to evaluate the global increase of efficiency in the management of interdependent urban networks.

Michele Minichino received his Electronic Engineering degree (Summa Cum Laude) from University of Naples in 1978. His main research interest is on methods, algorithms and tools for reliability, dependability and performance analysis of control and protection systems, computer-based systems, networked systems and (wired/wireless) communication networks. He has authored and co-authored more than 90 papers for international journals and conferences proceedings.

Angelo Nicotra joined the Sciemus' Power Team in May 2015. He is a postgraduate Power System Engineer and MSc in Electrical Engineering Cum Laude at Sapienza University of Rome. He developed his master thesis at ENEA on a decision support system for smart grid planning.

Marco Ranno received his Electrical Engineering degree from University of Catania in 2005. He is the Operation and Maintenance Manager of PV Plants at COGIPOWER.

Maurizio Reali received his Electrical Engineering degree from University of Rome in 2014. He developed his master thesis at ENEA on energetic performances of a smart grid.

Pasquale Regina is an Electrical Engineer skilled on energy production. Currently, he works in ENEA energy efficiency units on energy planning, energy efficiency, management end-use of energy and integration of renewable sources, smart grid and smart networks.

This paper is a revised and expanded version of a paper entitled 'Modelling interdependent urban networks in planning and operation scenarios' presented at DHSS 2014 International Defense and Homeland Security Simulation Workshop, Bordeaux, France, 10–12 September 2014.

## 1 Introduction

Modernised urban networks will ideally enable the integration of small distributed generation sources and will increase the customer's awareness, providing real time optimisation of network flows at the urban level, enabling interdependence and facilitating a multi-services approach. They will strengthen the links among the electricity carrier and gas, water and ICT infrastructures. The increased use of supervisory control and data acquisition (SCADA) ideally improves efficiency of modernised urban networks through a dynamic optimisation of their operations and resources. Modernisation of urban networks is a big long term challenge, for social, economic and technical reasons and it is far from being realised. Nowadays, even the term 'smart grid' has still to find a proper definition that fully includes its aspects of innovation and efficiency. An extensive use of comprehension and of models at an adequate level of granularity, is needed to support such a modernisation process (Alonge, 2014).

This paper proposes a cross-domain methodology to model and evaluate efficiency indicators of a medium voltage/low voltage (MV/LV) smart grid and its SCADA, interdependent, with water and gas networks. Models predict efficiency by

a adding to the main sources of each network, sources belonging to the other networks

b looking at the active components of water and gas networks energised by the electrical grid

c considering the main functionality of SCADA, the nervous system of each network, in optimising network behaviour.

Models have ideally to include SCADA functionalities, network interdependencies (at physical and ideally at geographical, cyber and organisational layers) energy efficiency and their degradation due to (natural, technological and malicious) adverse events (Ciancamerla, 2011).

The methodology, the models and the results have to be then extended and instantiated on the modernisation of the urban networks of the city of Catania, within the MIUR funded research project SINERGREEN. Such models will ideally provide knowledge and algorithms to feed a near real time decision support system for urban network utilities, local generation utilities, network customers, local authorities and regional civil protection.

## 2 Modelling approach

To build consistent models, a three steps approach has been pursued.

In the first step, we built a basic model of each network, with the multifold aim of selecting adequate simulation platforms, identifying the main parameters, characteristics and performance indicators of each network, accounting the indications of the Italian agency authority for electricity, gas and water (AEEGSI). We assume a scenario which includes a minimal topology of each physical network, enough to investigate solutions of local generation, load shedding, detection of natural, technological and malicious contingencies and their mitigation, by means of network reconfiguration performed by its SCADA. The topology consists of two (electricity, water or gas) feeders, each one feeding its subnet. In normal operative conditions the two subnets are separated from each other by two normally open tie switches. Each subnet delivers the physical flow to different (public, commercial, industrial) types of loads/passive customers network by means of physical trunks, connected one each other by normally close flow breakers. Tie switches, flow breakers and protection breakers at feeder, are remotely controlled by SCADA. SCADA, by means of its remote terminal units (RTU) which monitor the status of the physical network, implements load shedding, network reconfiguration upon contingencies (Bobbio, 2010).

In the second step, we consider an actual smart grid connected to photovoltaic (PV) plants of different power and location.

In the third step, we will consider electrical generation sources coming from the interdependent gas and water networks (i.e., gas co-generator and mini-hydro) and storage devices (i.e., electrical batteries, water and gas tanks). In such a step, the model of the actual smart grid and the basic models of gas and water networks will be interacting as a whole integrated model.

In this paper, we present the main results of the first two steps and discuss the main concepts of the third step.

We are investigating, step by step, energy efficiency indicators of the electrical grid on variation of location and power of distributed sources, electrical storage and other electrical distributed sources supported by gas and water network. The integration of renewable sources may affect grid stability, in terms of voltage and frequency that may lead to disturbances, devices anomaly, increased cable losses up to large black out scenarios. For example, intermittent cloud covering photovoltaic panels results in an intermittent electricity production that may cause grid voltage and frequency variations and, in turn, quality degradation of electricity to customers and even early failures of equipments. To mitigate such effects, energy storage systems (ESS), supply or absorb electrical power to compensate changes in solar irradiance, faster in time than the electrical power provided by conventional generators. In practice, the ESS dampen the quick variations of power from the PV and the degree of smoothing can be adapted to various applications. Our final models will ideally investigate how slower variation of electrical power could be mitigated by means of electrical generation by adequate gas and water network devices. That would reduce ESS number of charge/discharge cycles and then extends ESS life. Models provide knowledge to investigate control strategies, optimal location and power of distributed generations and ESS, with the aim of maximising energy efficiency of an actual smart electrical grid by using electrical generation devices fed by gas and water network. Particularly, to mitigate the instability of the electrical network due to renewable sources and optimise its efficiency, the adjustment of electrical loads belonging to the interdependent water and gas networks will be taken into account. For instance, in the hours of electrical power surplus or high load, water network could be temporarily reconfigured by including/excluding a certain number of pumps to increase/reduce the electrical load, relaying on gravity to provide water to customers. In case of electrical power surplus, it can be converted into potential energy by pumping water into storage tanks. Similarly, the distributed cogeneration installations, powered by gas network, may mitigate the impact of the intermittent, non-programmable renewable energy sources on the stability of the electricity network.

Starting from the above requirements, models of smart grid, water and gas urban networks and their interdependencies are under development, at the adequate level of granularity and abstraction, also in presence of contingences by means of an advanced simulation environment. A good compromise between particular and general models shall be found.

Figure 1 shows the simulation environment, which is constituted by:

1 specific domain simulators and transversal simulators, based on equations domain, able to generate data and status of the physical layer of each urban network, plus

2 event-based simulators which may properly represent SCADA functionalities and network operational layer

3 a contingency generator to inject natural, technological and malicious adverse events in networks and SCADA models.

**Figure 1** Simulation environment (see online version for colours)

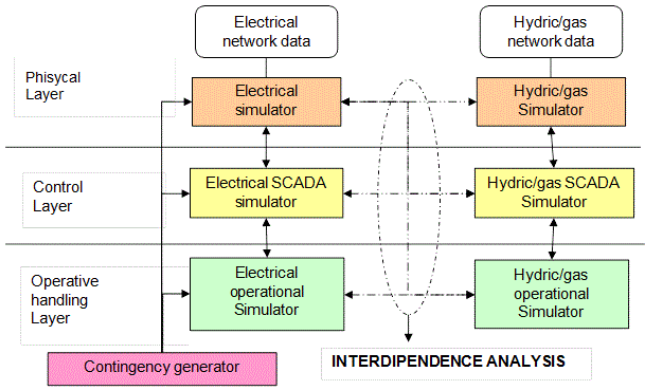


## 3 Planning and operation scenarios

Table 1 shows the main planning and operation scenarios of the smart electrical grid for different subjects.

The integration of local generation sources, due to high variability in producing energy which may cause power flow inversion (i.e., from HV/MV transformer to HV network), thermal overload and increment of joule losses of electrical trunks and voltage variations.

Initial models representing the behaviour of the electrical grid in some of such scenarios have been discussed in Alonge (2014).

Currently, the gas network is, and it is managed as, a passive network. The most prevalent topology for the gas distribution network consists of a simple mono feeder, branched tree type, with one-way flow from the first gas Pressure Regulating Station (PRS), to the final gas Pressure Regulating Installation (PRI). In large urban centres with industrial districts, the number of PRS increases according to load and pressure requirements and to a proper and optimal network balance. The stations are also interconnected with each other to create a meshed, reconfigurable network. On particular conditions or on critical faults, an inversion of gas flow may occur in some sections of the network, causing pressure reduction and, in some extreme cases, even the 'extinguishing of flame'. In near future, European technical standards will regulate the injection of bio methane local production into natural gas distribution networks, within safety, reliability, flow and operating pressure network constraints (D.Lgs 28/2011). As a consequence, similar to the electrical smart grid, the gas smart grid is thought of as an active network, in which the two-way gas flow is possible in any part of the network and the consumer may also become a producer. Demand side, network balancing, consumer/producer profiles, will be managed by means of an intensive use of remote monitoring and central control commands based on ICT technology. Although at a reduced speed compared to the electrical grid, even the gas network is undergoing throughout deep transformations and evolutions, leading the current passive gas network to become a smart one. Such a reduced speed is mainly due to the different nature of the energy vector, which in case of electricity consists of electrical cables, that are also used to transmit field data and commands, differently from the gas network that need a further carrier to transmit field data and commands. Such an innovation will transform the current passive gas network into an active network, with bidirectional gas flows and that will change its planning and operation scenarios. Even for the gas network there is a strong demand variability between consumption and supply by the distribution system gas operator (DSO). The gas demand is variable according to the season (winter/summer), daily temperatures, the production cycle of industrial users, and the demand for electricity and thus it presents a variable consumption profile. Gas network physical balance implemented by DSO, concerns the optimal management of gas flows on the network to ensure safe and reliable network operation based on the actual gas flow demand.

**Table 1** MV smart grid scenarios

| *Subject* | *Planning scenario* | *Operation scenario* |
|---|---|---|
| Distributed system operator | Power flow inversion from HV/MV transformer to HV network | Power flow inversion from HV/MV transformer to HV network |
| | Thermal overload of MV trunks | Outage due to failure or maintenance and fault isolation and system restoration (FISR) |
| | Voltage variation over ± 10% of nominal value | Voltage variation over ± 10% of nominal value |
| | Short circuit currents at the active user nodes | |
| Renewable energy utility | Long distance between renewable plant and MV grid connection point (increased connection costs) | Renewable plant disconnection from MV public utility due to failure or maintenance |
| | | Renewable plant disconnection due to voltage variation over ± 10% of nominal value |
| Passive customer | | Voltage variation over ± 10% of nominal value |
| | | Outage due to failure or maintenance |

Typically, a water distribution network has no active users and the flow proceeds normally from the feeders to the consumers. Undesirable situations may occur, as fault scenarios, and then network reconfiguration could be needed to limit flow degradation to customers and even disruptions of network elements and devices. The focus here is the efficiency and interdependency and not water contamination. However, temporal duration of water inside the pipes has to be taken into account, in compliance with law requirements of water for human consumption (i.e., Legislative Decree No. February 2, 2001, n. 31 et seq.). Water network enables the transport and the regulation of water flow and pressure by means of elements, such as pipes, valves, fittings, storage systems, devices for regulation and control (SCADA) and of machines (i.e., pumps) to provide energy to move the water. Pumps transfer the energy, supplied from the electrical grid, to water and represent for the grid a positive load (power consumption). In the view of increasing energy efficiency, valves for water pressure reduction can be substituted by mini-hydro. Mini-hydro exploits the presence of a hydraulic jump to recover energy, otherwise dispersed in friction, and fed back the electricity grid, representing for the grid a negative load (power generation). A further and most important aspect for energy efficiency is the presence of water reservoirs, localised in appropriate areas of the territory, which constitute buffers to stabilise water flow and pressure. Urban reservoirs may supply water for short periods (5–6 h), to satisfy user contract requirements, and to help in balancing power generation and consumption of the interdependent electrical grid, by means of the disconnection of the electrical loads, represented by water pumps, in case of electricity demand greater than electricity production. Similarly, in case of electricity demand lower than the electricity production, water pumps may be re-activated, so increasing the load of electricity grid. The management of the mini-hydro and the water reservoirs, proposed here, needs to account the functionality of SCADA to optimise pump switching procedure.

In water network planning and operation scenarios, different aspects have to be considered, such as:

1 physical-chemical-biological requirements for drinking water (i.e., Legislative Decree no. February 2, 2001, n. 31 et seq.), which implies flow speed greater than 0.5 m/s and, in any case, water residence times (age) in the pipes of less than ten hours

2 overpressure and its consequences, water hammer (permissible tolerance range according to the manufacturer's specification)

3 speed in the pipes below 1.5 m/s and avoid abrupt operations that may generate harmful pressure waves.

## 4 Interoperability and heterogeneity of networks and simulators

In modernised urban networks, the electrical smart grid, including, by itself, heterogeneous ICT-based systems, such as IACS and SCADA, is expected to interoperate with other heterogeneous networks, such as gas and water network, each one relying on its own SCADA system. Challenging issues such as performance, safety and security of the networks arise, including SCADA cyber security.

Simulation environments to represent such challenging issues need the cooperation of specific domain simulators, based on equations domain, able to generate data and status of the physical layer of each urban network, and event-based simulators for representing SCADA functionalities and network operational layer, as chosen in our modelling approach (Figure 1). In fact, current domain simulators, such as electrical load flow simulators, and gas and water network simulators, typically do not model SCADA functionalities, communication protocols, or even SCADA traffic patterns. On the other hand, the operating mode of each urban network, specially of the smart grid, has an impact on its own SCADA system. Thus, such an integration of physical and ICT components of the operational urban networks requires similarly integrated simulation frameworks. The use of standards-based approaches (HLA, IEC 61850, CIM, etc.) ideally facilitates the interoperability of different simulators that are acquired or developed over time, as well as the exchange of simulation models. However, the implementation of standards by themselves does not grant the adequate implementation of any modelling issue, such as the efficiency computation of interoperable but heterogeneous physical networks and their SCADA.

For such a reason, here, we are investigating a unified modelling framework, which relies on a hybrid modelling approach, in which actual physical devices, emulators and heterogeneous simulators (as agent-based, discrete event, domain and traversal simulators) co-exist and are logically composed to represent the operational urban networks and their SCADA.

Particularly, flow efficiency computation requires a deep knowledge of the physical, control and operational layers of urban networks (Figure 1). The physical layer and a part of the operational layer are going to be represented by means of domain simulators, such as PSS-SINCAL of Siemens, Epanet and Neplan. The control layer and the complementary part of the operational layer that regards SCADA systems functionalities, communication protocols, or even SCADA traffic patterns, are going to be represented by means of NS2 open source simulator and via MATLAB-Simulink. Contingency generators, i.e., to represent cyber-physical threats and the propagation of their effects on SCADA devices, are going to be modelled by threats generators, emulation or actual mock ups of the related ICT-based devices.

Currently just offline communication among such simulators has been implemented, by means of Excel and HTML exchange formats.

## 5 Basic urban networks models

We present and discuss three basic models: MV smart grid, gas network and water network models. The aim of each model is twofold:

1 to validate simulator accuracy by cross-checking model results of the same network by two different simulators

2 to investigate mini-hydro, water reservoirs and gas co-generators as components of the basic water and gas networks.

A relevant aspect is the validation of the simulators and their adequate selection within the modelling process. To address it, we are using domain simulators, such as PSS Sincal, EPANET and Neplan, which can faithfully represent the physical infrastructure and compute its parameters, combined with the use of transversal simulators, such as MATLAB and Simulink, which can more easily include the physical network and its SCADA in a single model. Moreover, MATLAB and Simulink may easily represent network interdependencies at physical, logical and geographic levels. The main parameters of mini-hydro and gas co-generators used in the models are reported in Tables 2 and 3.

Particularly, a mini-hydro of 4.5 MW, fed by water network, provides electrical energy to the MV sub-grid and two co-generators, fed by gas network, provide 20 kW to the LV subgrid and 400 kW to the MV sub-grid.

**Table 2** Mini-hydro parameters

| | |
|---|---|
| Turbine | 1 × Francis |
| Height ($H_0$) | 65 (m) |
| Flow (Q) | 0.01–0.015 ($m^3/s$) |
| Installed power | 4.5 (MW) |
| Yield (η) | 70% |

**Table 3** Gas co-generator parameters

| *Electrical power (kW)* | *Thermal power (kW)* | *Electrical yield (%)* | *Thermal yield (%)* |
|---|---|---|---|
| 20 | 39 | 32.23 | 62.90 |
| 401 | 549 | 38.08 | 52.14 |

### *5.1 MV smart grid*

MV smart grid model implements:

- two HV/MV substations, with their MV backbones and protection breakers
- passive users: loads
- active users: renewable generators
- prosumers: active/passive users
- a LV backbone, with its own set of devices and active/passive users.

Two different models of the same basic MV electrical grid have been built. Figure 2 shows the model and the load flow computation by means of PSS-Sincal simulator. Figure 3 shows the model of the same grid built by Simulink.

**Figure 2** Basic MV grid model by PSS Sincal (see online version for colours)

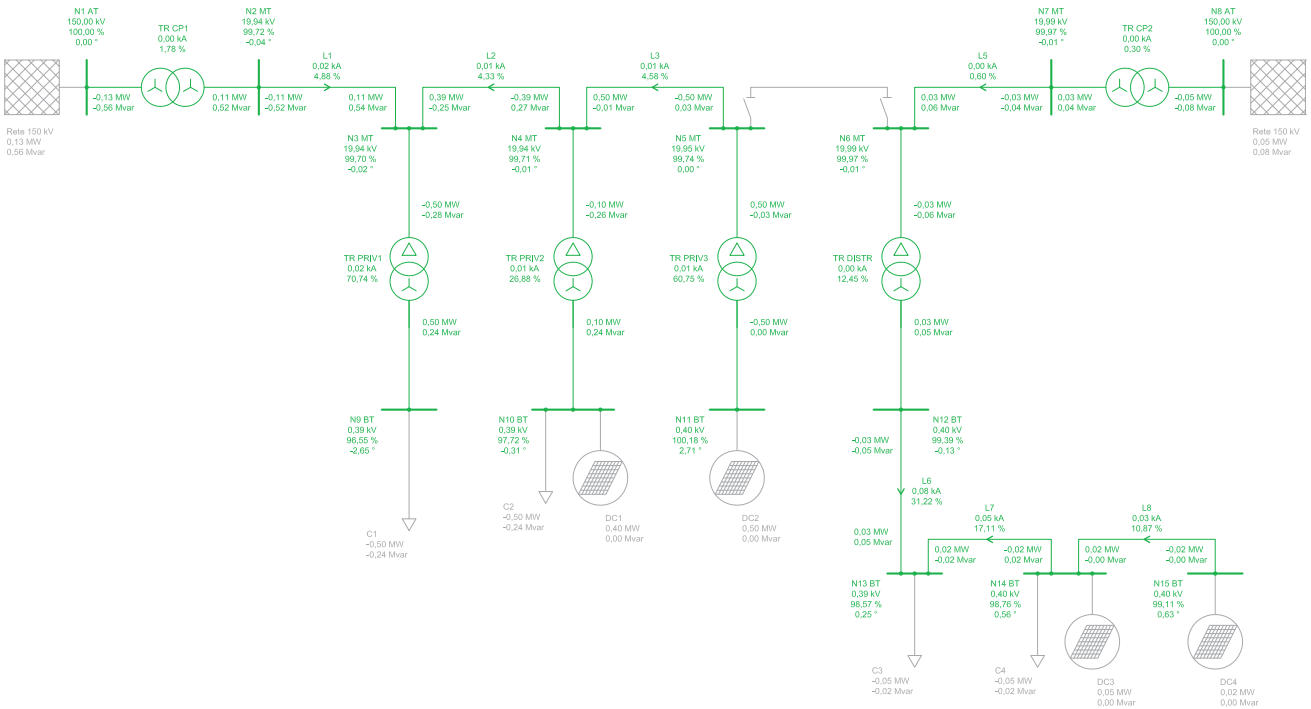

**Figure 3** Basic MV grid model by Simulink (see online version for colours)

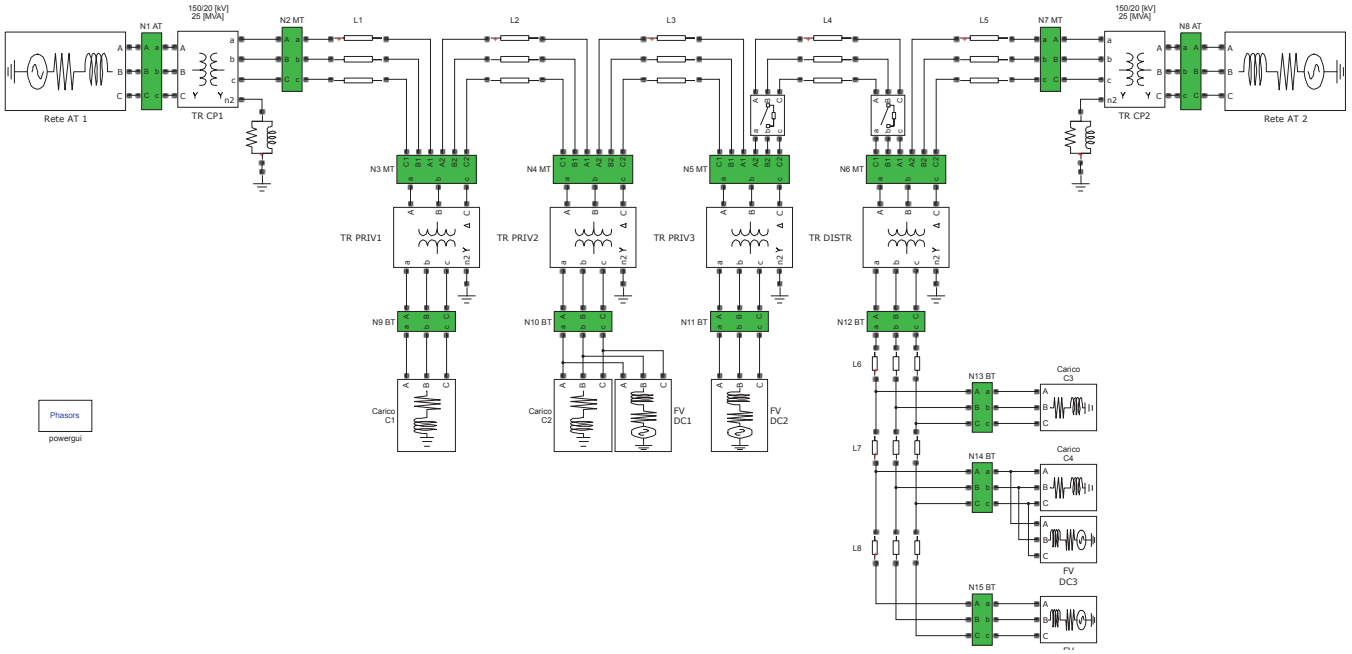


**Table 4** Transformers parameters

| *Transformers* | *TR CP1* | *TRCP2* | *TR PRIV1* | *TR PRIV2* | *TR PRIV3* | *TR DISTR* |
|---|---|---|---|---|---|---|
| Avvolgimento | Yyn | Yyn | Dyn | Dyn | Dyn | Dyn |
| V1n[kV] | 150 | 150 | 20 | 20 | 20 | 20 |
| V2n[kV] | 20 | 20 | 0,4 | 0,4 | 0,4 | 0,4 |
| Sn[kVA] | 25000 | 25000 | 630 | 800 | 630 | 400 |
| Smax[kVA] | 32500 | 32500 | 820 | 1040 | 820 | 520 |
| fn[Hz] | 50 | 50 | 50 | 50 | 50 | 50 |
| Vcc%[p.u.] | 13 | 13 | 6 | 6 | 6 | 6 |
| Pcc%[p.u.] | 0,42 | 0,42 | 0,76 | 0,75 | 0,76 | 0,81 |
| Po[kW] | 22,75 | 22,75 | 0,68 | 0,80 | 0,68 | 0,52 |
| Io%[p.u.] | 0,2 | 0,2 | 1,8 | 1,65 | 1,8 | 1,9 |

Electrical parameters of grid elements and their values, including the ones of photovoltaic sources, partially reported in Tables 4 and 5, are realistic ones.

**Table 5** Generators and loads parameters

| *Generator* | *DC1* | *DC2* | *DC3* | *DC4* |
|---|---|---|---|---|
| P[kW] | 400 | 500 | 50 | 20 |
| Q[kVar] | 0 | 0 | 0 | 0 |
| *Load* | *C1* | *C2* | *C3* | *C4* |
| P[kW] | 500 | 500 | 50 | 50 |
| Q[kVar] | 242 | 242 | 24,2 | 24,2 |

The comparative results, in terms of voltages on different nodes of the grid, and computation errors of the power load flow, between PSS-Sincal and Simulink, are shown in Table 6.

**Table 6** Simulink versus PSS-Sincal results

| *Voltage (kV)* | *Simulink* | *PSS SINCAL* | *Error %* |
|---|---|---|---|
| N1 AT | 150.000 | 150.000 | 0.00 |
| N2 MT | 19.946 | 19.944 | 0.01 |
| N3 MT | 19.941 | 19.939 | 0.01 |
| N4 MT | 19.944 | 19.942 | 0.01 |
| N5 MT | 19.949 | 19.948 | 0.01 |
| N6 MT | 19.995 | 19.993 | 0.01 |
| N7 MT | 19.996 | 19.994 | 0.01 |
| N8 AT | 150.000 | 150.000 | 0.00 |
| N9 BT | 0.386 | 0.386 | 0.00 |
| N10 BT | 0.391 | 0.391 | 0.00 |
| N11 BT | 0.401 | 0.401 | 0.00 |
| N12 BT | 0.398 | 0.398 | 0.00 |
| N13 BT | 0.395 | 0.394 | 0.25 |
| N14 BT | 0.396 | 0.395 | 0.25 |
| N15 BT | 0.397 | 0.396 | 0.25 |

Errors are very limited, less than or equal to 0.25%. Then, we conclude that PSS Sincal and MATLAB-Simulink can be safely used, from the point of view of their computational accuracy.

The full description of the basic MV smart grid model, the load flow computation in normal operation and the implementation of the fault isolation and system restoration (FISR) procedure is reported in Alonge (2014).

### 5.2 Gas network

The basic gas network has two feeders: two interconnected first gas PRS feed portions of a branching network, to supply different types of users and/or PRI:

1 Industrial consumers (IC), directly connected to medium pressure network or thermal power plants.

2 Home consumers, connected to final gas pressure regulating groups $PRI_f$ in which the upstream pressure of 5 bar is reduced to 23 mbar (each PRI may feed even hundreds of consumers).

3 Small industrial $PRI_i$ (upstream pressure is reduced to a range between 50 and 200 mbar). In the network, a combined heat and power generator (CHP) 401/549 kW with consumption of 105.3 $Nm^3/h$ at 200 mbar has been included.

4 Specific consumers with specific values of pressure – flow $PRI_u$. An example is a cogeneration unit (in the model a CHP 20/39 kW with consumption of 6.2 $Nm^3/h$ at 50 mbar).

5 Biomethane1 that identifies the 'active user' type, which enters biomethane into the natural gas distribution network.

Figure 4 shows load flow in normal operation by Neplan. Data of each section (diameter, thickness, length, coefficient of roughness, friction coefficient lambda linked to relative roughness and Reynolds number) are DSO compliant.

In normal operation, the network is balanced, and its parameters such as gas pressure, flow, pressure drop and speed are measurable or calculable for each network component.

Network reconfiguration, in case of contingencies/faults, is possible by acting on a normally open branch. Assuming a failure in one of the components of the network, it is possible to isolate the failure and perform a reconfiguration of the network by means of remote controlled valves in order to ensure continuity of operation. FISR procedure may change depending on failure location. For example, if the failure affects the first gas PRS, it is possible to act on the upstream and downstream valves to isolate it. Supply continuity is ensured by reconfiguration based on meshing of PRS stations. If the failure affects a middle network section, that would isolate an entire trunk (such as the point '1 *Failure*' of Figure 5), it is possible to operate the upstream and downstream valves of the affected section and to act on normally closed valves to make a network reconfiguration (such as the point '2 *Reconfiguration*' of Figure 5). In the portion indicated as '3 *Inversion*' in Figure 5, there is a gas flow inversion.

At the same time, it can be seen that the first gas PRS is subjected to an overload, however, within the limits of design capacity. The different colours of A and B pipes indicate the criticality of the network in such pipes because they do not meet design constraints of pressure and/or speed of the gas inside the pipes.

The pressure regulators, the loads and the input parameters and values of gas-electricity interconnection devices are respectively reported in Tables 7, 8 and 9.

Network model has been built by means of Neplan and PSS Sincal and then load flow simulations were performed and compared. Figure 6 reports the load flow simulation results in normal operation, by PSS-Sincal.

**Table 7** Pressure regulators parameters and values

| *Pressure regulator* | *Pressure in [mbar]* | *Pressure out [mbar]* | *Note (type)* |
|---|---|---|---|
| CL75 | 74000 | 5000 | Pressure regulator station |
| CL76 | 74000 | 5000 | Pressure regulator station |
| CL78 | 5000 | 50 | Specific consumer |
| CL79 | 5000 | 50 | Specific consumer |
| CL80 | 5000 | 50 | Specific consumer |
| CL81 | 5000 | 200 | Small industrial |
| CL82 | 5000 | 750 | Small industrial |
| CL84 | 5000 | 23 | Home consumer |
| CL85 | 5000 | 23 | Home consumer |
| CL86 | 5000 | 1000 | Small industrial |
| CL90 | 5000 | 23 | Home consumer |

**Table 8** Load parameters and values

| *Load* | *Pressure [mbar]* | *Flow consumption [m/h]* | *Note* |
|---|---|---|---|
| C26 | 5000 | 750 | Eq CCGT |
| C30 | 200 | 150 | CHP 1 |
| C32 | 5000 | 500 | Eq CCGT |
| C34 | 50 | 2000 | |
| C40 | 23 | 1000 | |
| C42 | 50 | 10 | CHP 2 |
| C52 | 50 | 50 | |
| C60 | 750 | 50 | |
| C61 | 23 | 1000 | |
| C62 | 23 | 10000 | |
| C63 | 1 | 250 | |

**Table 9** Gas-electricity interconnection devices

| *LOAD* | *CHP* | *Electrical power (kW)* | *Thermal power (kW)* | *Flow consumption ($m^3$/h)* | *Pressure (Mbar)* |
|---|---|---|---|---|---|
| C30 | CHP 1 | 401 | 549 | 105.3 | 200 |
| C42 | CHP 2 | 20 | 39 | 6.2 | 50 |

**Figure 4** Load flow of the gas network in normal operation by Neplan (see online version for colours)

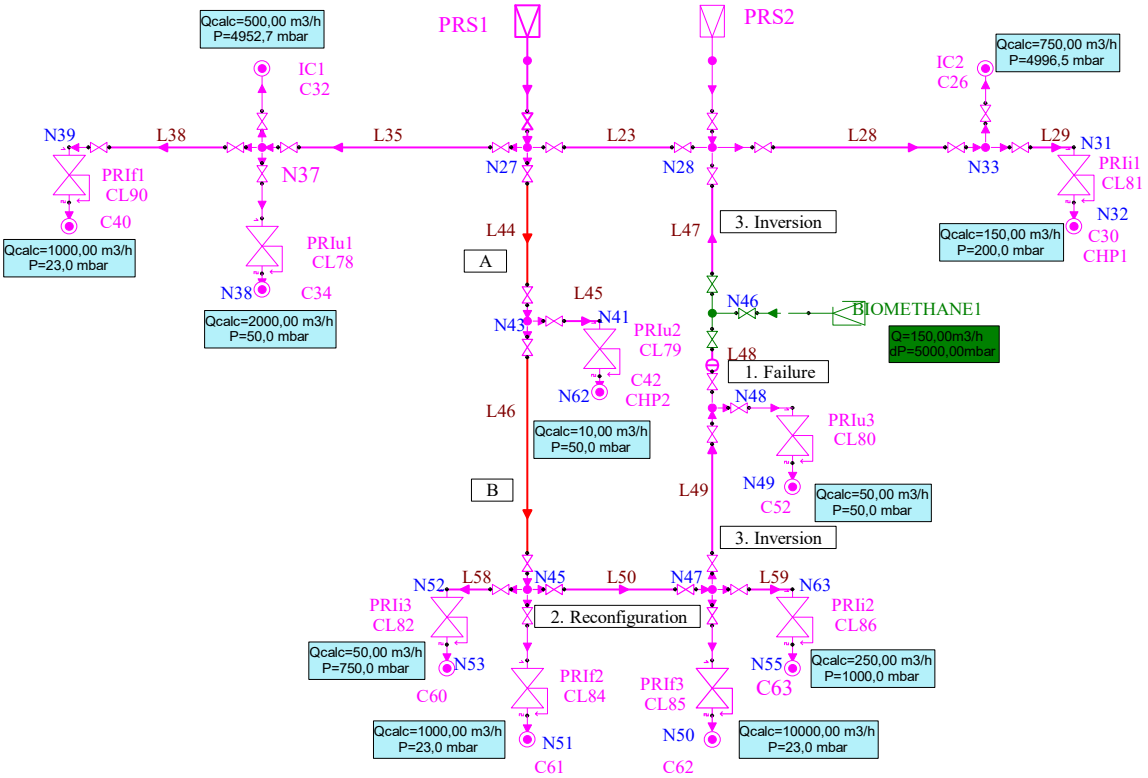


**Figure 5** Load flow of the reconfigured gas network by Neplan (see online version for colours)

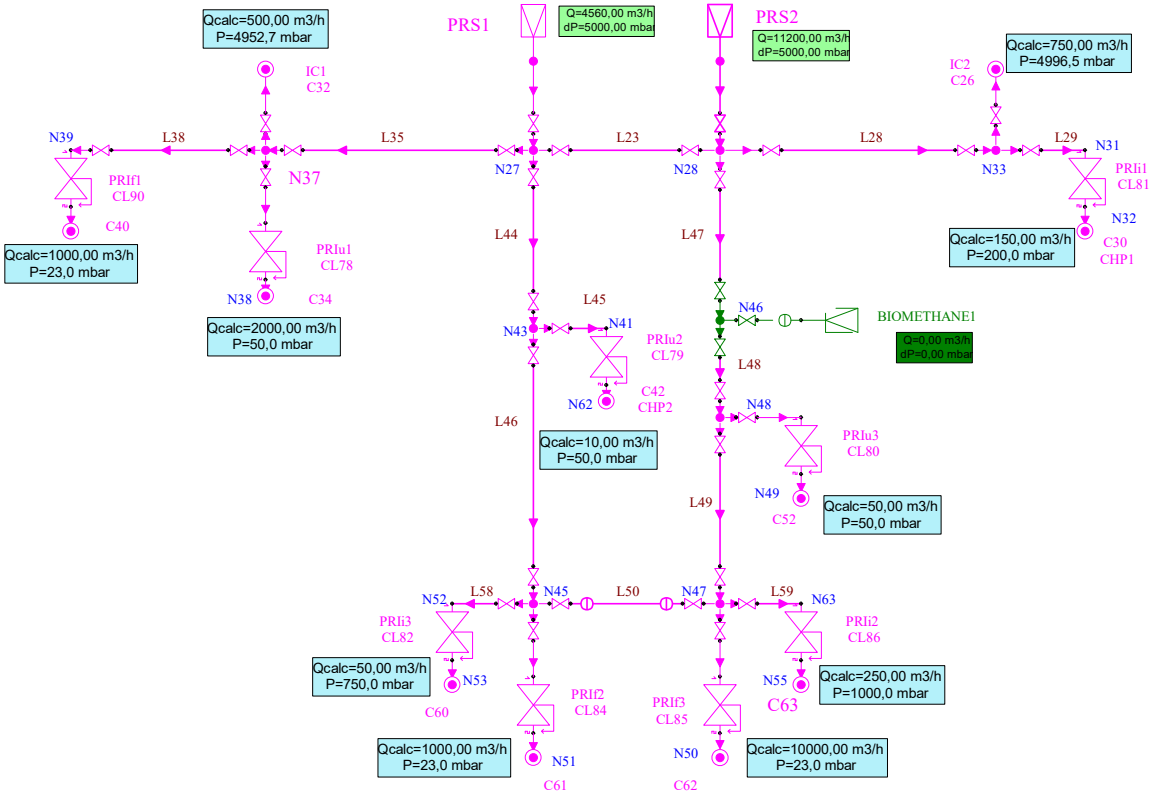

**Figure 6** Load flow model of the gas network by PSS Sincal (see online version for colours)

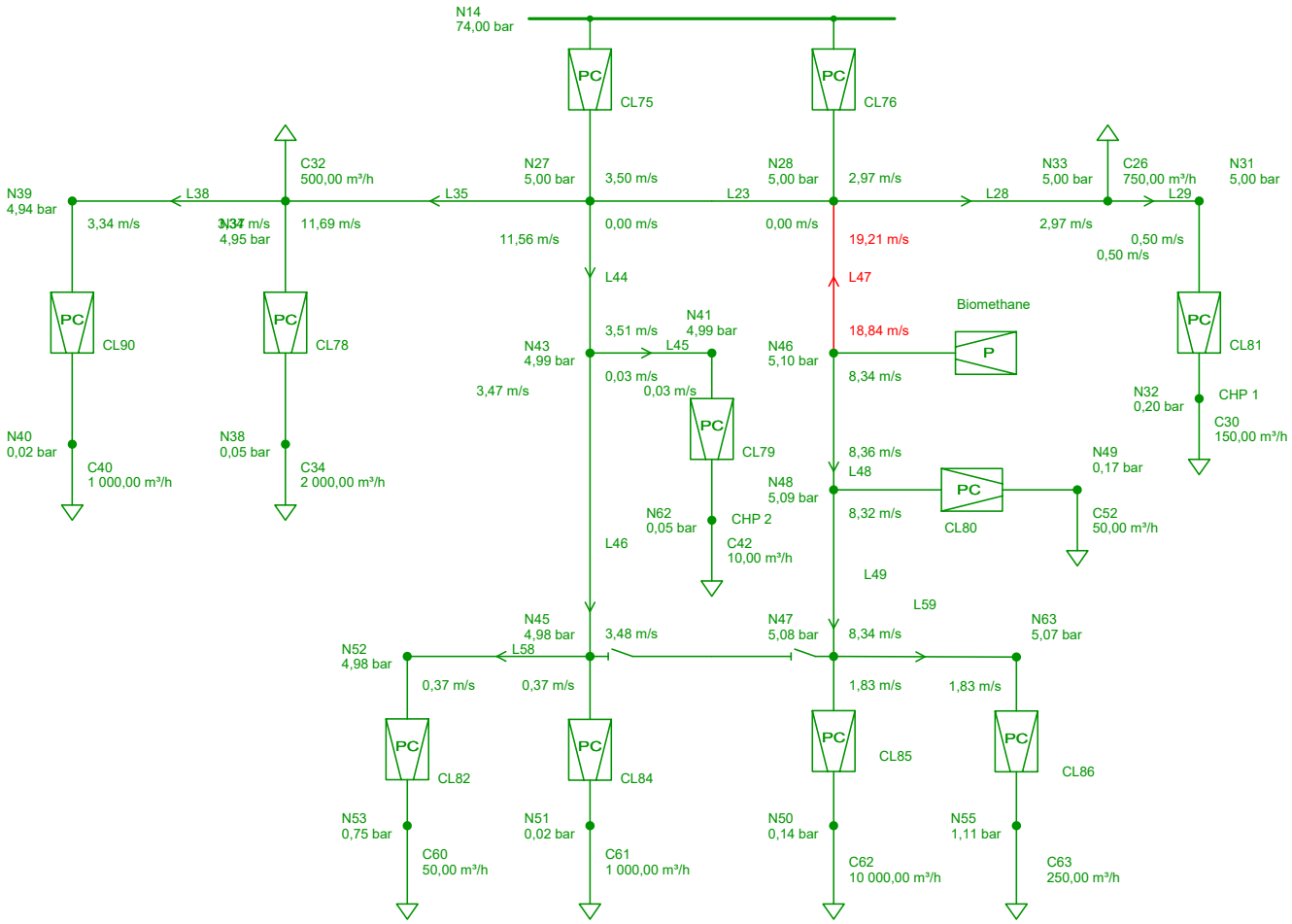


**Table 10** Neplan-PSS Sincal pressure differences

| *ID Neplan* | *ID Sincal* | *Pa Neplan [mbar]* | *Pa Sincal [mbar]* | *ΔP [mbar] N-S* | *ε %* |
|---|---|---|---|---|---|
| N-175685-N27 | N27 | 5000 | 5000 | 0 | 0 |
| N-175446-N28 | N28 | 5000 | 5000 | 0 | 0 |
| N-175496-N33 | N33 | 4996,506 | 4995,998 | 0,508 | 0,01 |
| N-175751-N37 | N37 | 4952,686 | 4945,299 | 7,387 | 0,15 |
| N-175969-N43 | N43 | 4991,288 | 4990,003 | 1,285 | 0,03 |
| N-175922-N45 | N45 | 4983,678 | 4981,268 | 2,41 | 0,05 |
| N-178620-N46 | N46 | 4982,817 | 4980,173 | 2,644 | 0,05 |
| N-175905-N47 | N47 | 4961,08 | 4955,061 | 6,019 | 0,12 |
| N-176006-N48 | N48 | 4971,334 | 4966,911 | 4,423 | 0,09 |
| N-177334-N62 | N62 | 50 | 50,00292 | –0,003 | –0,01 |

Operating parameters, such as pressure and flow rate are computed at each node and branch of the network. Also, flow direction is indicated for each branch.

The impact of the active user biomethane1 on the flow rate and direction has been investigated too. With a flow rate of 150 $m^3/h$ at 5 bar pressure, the biomethane1 implies a reversal of flow in the branch L47, with gas flow rate above the design limit. Tables 10 and 11 show the main results of load flow by means of the two simulators, respectively in terms of pressure, at the main nodes and load loss and flow rate at each branch. Also the computational differences are shown. Computation errors between the two models are very limited, less than or equal to 0.15%. We can conclude that Neplan simulator underestimates load losses compared to the Sincal simulator within negligible error limits (0.15%). Table 11 shows that higher losses are located in higher flow rate branches and also in branches at the dimensioning limit for which gas speed is near to the imposed constraints.

**Table 11** Neplan-PSS Sincal load loss and flow rate

| *ID Neplan* | *ID Sincal* | *J [mbar/km] Neplan* | *v [m/s] Neplan* | *J [mbar/km] Sincal* | *v[m/s] Sincal* | *ΔJ [mbar/km] N-S* | *ΔV [m/s] N-S* |
|---|---|---|---|---|---|---|---|
| L-178226-L23 | L23 | 0 | 0 | 0 | 0 | 0 | 0 |
| L-177884-L28 | L28 | 34,94 | 2,39 | 40,01962403 | 2,97187 | –5,08 | –0,582 |
| L-177889-L29 | L29 | 1,02 | 0,4 | 1,11859548 | 0,49571 | –0,099 | –0,096 |
| L-177985-L35 | L35 | 525,71 | 9,34 | 607,7891815 | 11,5573 | –82,079 | –2,217 |
| L-178010-L38 | L38 | 43,43 | 2,67 | 49,94655976 | 3,3386 | –6,517 | –0,669 |
| L-178050-L44 | L44 | 48,4 | 2,81 | 55,53709992 | 3,5002 | –7,137 | –0,69 |
| L-178045-L45 | L45 | 0 | 0,03 | 0,005410692 | 0,03309 | –0,005 | –0,003 |
| L-178204-L46 | L46 | 47,57 | 2,79 | 54,59706655 | 3,47413 | –7,027 | –0,684 |
| L-178644-L47 | L47 | 114,55 | 6,84 | 132,1795678 | 8,50285 | –17,63 | –1,663 |
| L-178661-L48 | L48 | 114,83 | 6,85 | 132,6192774 | 8,5367 | –17,789 | –1,687 |
| L-178209-L49 | L49 | 113,93 | 6,83 | 131,6675355 | 8,51794 | –17,738 | –1,688 |
| L-178179-L58 | L58 | 1,01 | 0,3 | 1,088827347 | 0,37288 | –0,079 | –0,073 |
| L-178184-L59 | L59 | 23,81 | 1,5 | 27,16894288 | 1,87426 | –3,359 | –0,374 |

**Figure 7** Load flow of water network in normal operation by Epanet (see online version for colours)

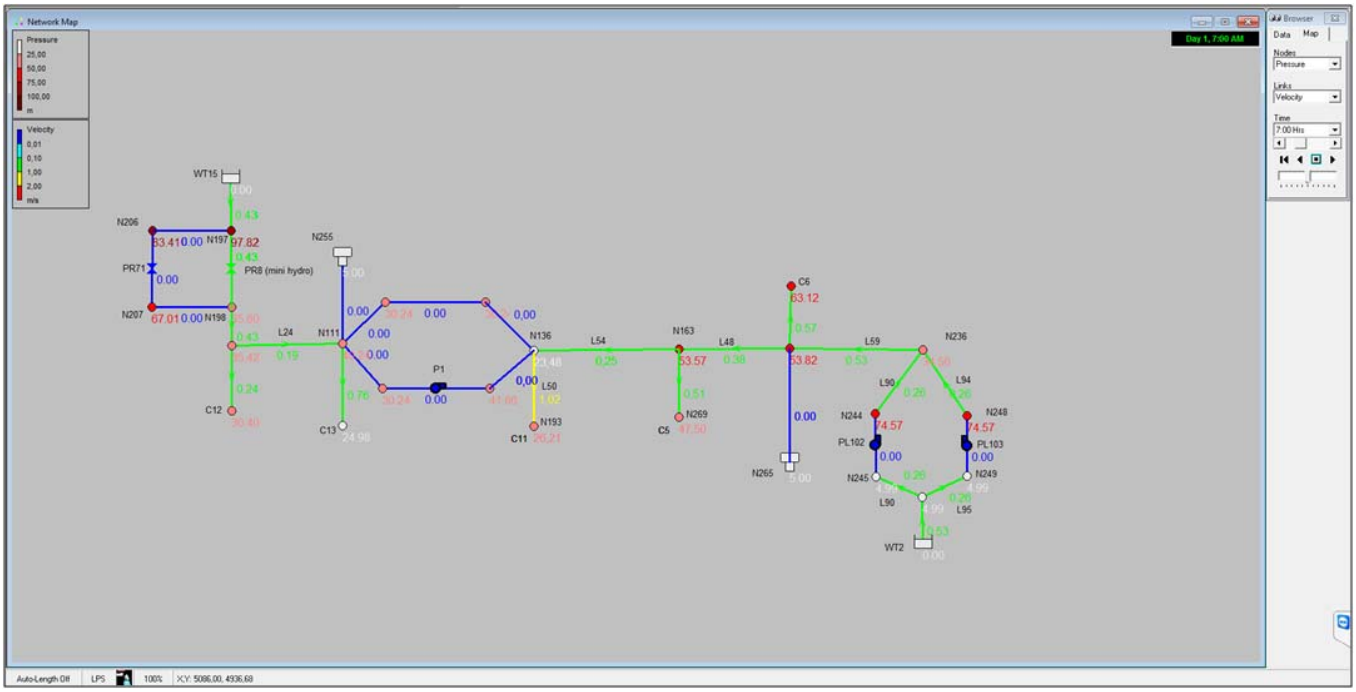


## *5.3 Water network*

The urban water network model has been developed by two different softwares: Epanet (Figure 7) and PSS Sincal (Figures 8 and 9). Both models implement:

- Two sources (WT15, WT2), each one able to feed alone the whole network, as in case of a failure scenario. In normal operation (Figures 7 and 8), the left branch is fed by reservoir WT15, while the right branch is fed by reservoir WT2. PL10 pump is normally switched off so that the left branch results disconnected from right one, and the links that connect them to the rest of the network are normally closed. PL102 and PL103 pumps are normally active, and allows the right branch to be fed. These pumps refilled the water tower WT99 in hours of low water demand, this often overlaps with hours of low electricity demand.
- Public, commercial, and industrial consumers (C12, C13, C11, C5, C6), for a district that serves about 10,000 inhabitants-equivalent, with an expected daily water requirement of 240 l/inhabitant • day.
- PR71 and PR8 valves, where PR71 is a pressure regulating valve (PRV) and PR8 represents a mini-hydro plant. During the period of maximum flow, with the considered hydraulic jump, it is possible to produce electric power [up to 6 (MW)]. In night hours, water consumption is reduced, and the mini hydro plant

is closed. Each link presents also the possibility to be open or to be closed.

- Two tanks, WT 99 and WT61 that are able to feed respectively, the left branch and the right one for a few hours. To do this, it is not necessary to use the pumps, because each tank is able to feed the branch by means of gravity. Normally, tanks are refilled when the load in the network is low as it typically occurs during the night.

In the left branch, there are the supply network (fed from source WT15), at high pressure (≈10 bar) and the distribution network at lower pressure (≈3.5 bar), separated by means of PR8 mini-hydro and PR71 valve. Mini-hydro is represented by a pressure regulating valve (PR8) that operates in parallel (as an alternative way) to the pressure regulating PR71 valve, since both have, as their ultimate effect, a decrease in the piezometric head of the fluid. The mini hydro turbine operates during the high water demand periods (daytime), and it is replaced by the regulating pressure valve PR71 during the low water demand. It is possible, in the case of failure of the source WT15, to feed the right branch of the network, with the activation of the pump PL10. The left branch can be fed from the WT2 tank and does not require the activation of additional pumps, since the water has sufficient energy to reach the users.

Figures 7 and 8 refer to a particular operating point, characterised by certain parameters of instantaneous water flow (it continuously varies during the day depending upon the water demand). In normal operation, the daily flow, between 7:00 and 8:00 a.m., in the left branch is 13.5 l/s while in the right branch is 16.5 l/s (the total flow rate for the power supply of the two branches is 30 l/s).

With an appropriate hydraulic jump (i.e., from 9.8 bar to 3.4 bar = 6.4 bar), the turbine provides about 6 (MW) of electrical power, considering an overall conversion efficiency, ηtot = 0.7, under the maximum flow rate. The right branch is powered using a lifting system with pumps working in parallel.

As an example of contingency, an outage of WT2 and WT15 is considered. To grant water to customers, the right and left branches of the network are reconfigured, see Figure 9. Customers are then respectively fed from WT99 and WT61 tanks, for a few hours before they become empty.

The difference between Epanet and PSS-Sincal in normal operation has been computed in terms of pressure and speed (and therefore flow rate). The speeds inside the pipes are identical, while the pressure in the nodes shows a maximum deviation of 0.67 bar in a single node, the edge of the network, as reported in Table 12 (1 bar = 10.197 metre column water [mcw]).

**Table 12** Epanet/Sincal pressure differences

| *ID* | *Pressure (bar)* | | | *Diff. (bar)* |
|---|---|---|---|---|
| | *Sincal* | *Epanet (mcw)* | *Epanet (bar)* | |
| N109 | 3.48 | 35.42 | 3.47 | 0.01 |
| N276 | 2.8 | 30.4 | 2.98 | –0.18 |
| N273 | 2.36 | 24.98 | 2.45 | –0.09 |
| N111 | 3.93 | 40.24 | 3.95 | –0.02 |
| N136 | 2.28 | 23.64 | 2.32 | –0.04 |
| N193 | 1.9 | 26.21 | 2.57 | –0.67 |
| N163 | 5.25 | 53.57 | 5.25 | 0.00 |
| N164 | 5.25 | 53.82 | 5.28 | –0.03 |
| N198 | 3.5 | 35.6 | 3.49 | 0.01 |
| N236 | 3.52 | 34.56 | 3.39 | 0.13 |
| N277 | 6.22 | 63.12 | 6.19 | 0.03 |

**Figure 8** Water network in normal operation by PSS Sincal (see online version for colours)

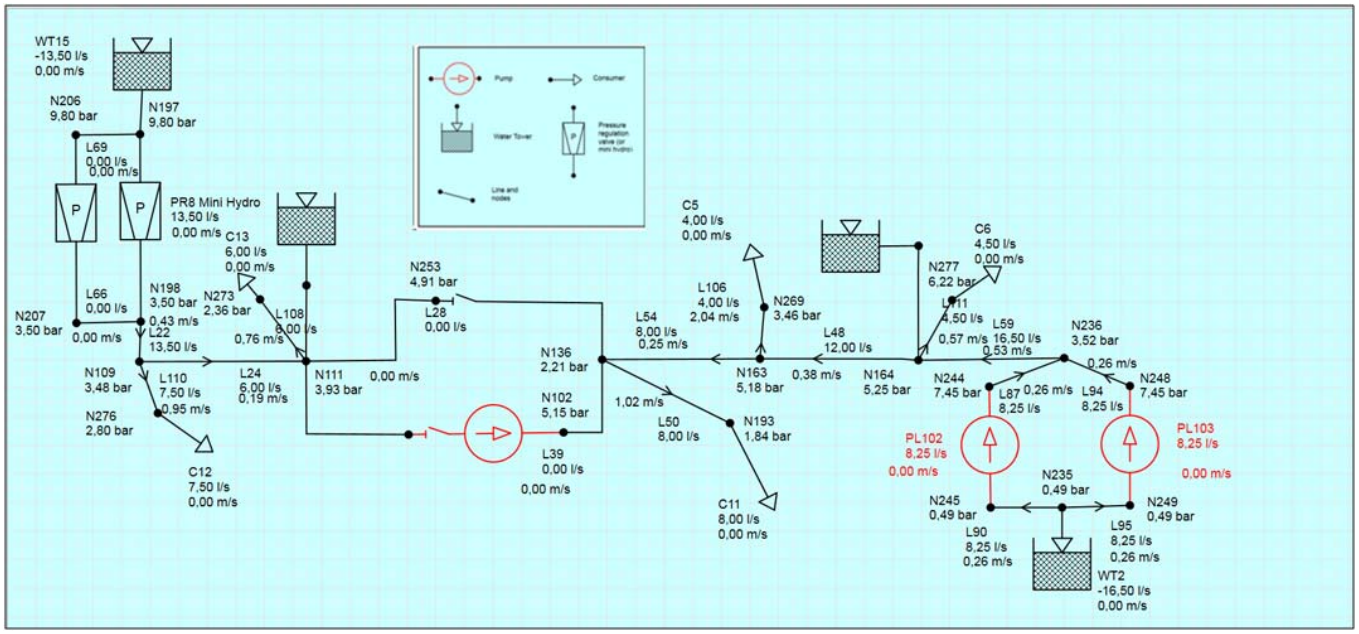

**Figure 9** Water network in failure scenario by PSS Sincal (see online version for colours)

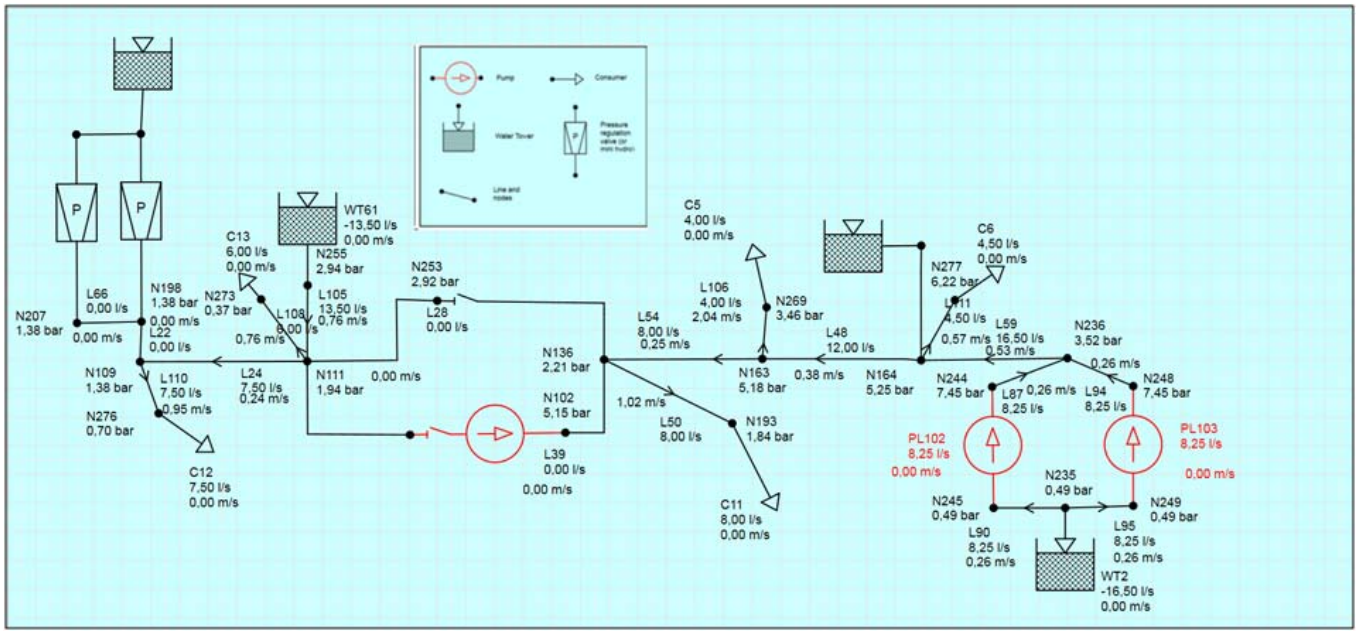


## 6 Computing energy efficiency

To compute the energy efficiency of interdependent urban networks, we pass throughout indicators of each single network. For the smart grid, three classes of efficiency indicators have been investigated: node, branch and statistics indicators. By node (single-phase/three-phase) we mean a point at which two or more terminals are connected, i.e., the MV busbar of primary substation or point of delivery of different kinds of users, such as consumers, prosumers and generators. Branch is intended as any electrical connection between two nodes. The first two indicators characterise the electrical grid parameters from DSO point of view, while the last one characterises prevision on electricity production and consume. Statistical indicators take into account:

1 the partition of load for kind of users

2 the production of electrical energy from renewable sources

3 covering hours and penetration coefficients of distributed generation.

To measure the impact of the variation of the size, location and storage of distributed generation on grid efficiency, we select indicators such as:

1 *hours of power inversion at node* (i.e., primary substation or transformer)

2 daily profile of power at transformer

3 loss of power at branch.

### *6.1 The actual smart grid*

As actual smart grid, a portion of the MV Enel Distribution grid, located at Carpinone, Isernia (Molise) (Enel, 2013) has been considered. Such a network is part of a pilot project funded by the Italian Authority of Electrical Energy and Gas (ARG/ELT 39/10) and it is considered the first national Smart Grid installation (http://www.autorita.energia.it/it/operatori/smartgrid.htm). The network is connected to the HV/MV substation of Carpinone. Such a substation is connected to the national transmission network (RTN) at 150 kV, throughout DM00 1-380404 node.

**Figure 10** The actual smart grid (see online version for colours)

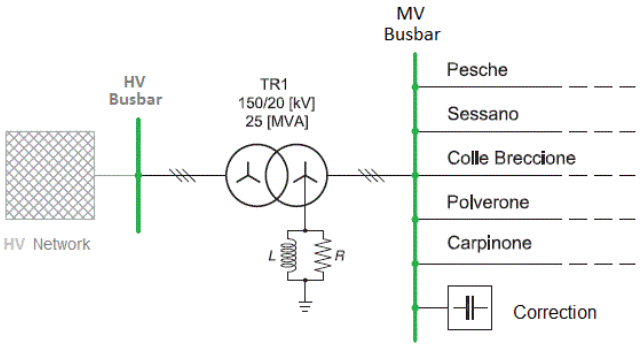


Figure 10 shows the actual smart grid. The MV section is fed at 20 kV. The connection scheme consists of a simple bus-bar. The transformer TR1 has the nominal voltage of 150 (kV) on the HV side and of 20.8 (kV) on the MV side, at the nominal power of 25 MVA. The transformer is equipped with a tap changer mechanism, which enables voltage regulation of the MV bus-bar according to load variation. The neutral of the MV transformer is connected to the ground by a Petersen coil compensation. The value of the reactance is such that, when an earth fault occurs, the current through the reactance balances the capacitance current flowing through the fault, so that any trend to electrical arc is suppressed. In Table 13, are reported some of the variables that characterise the users, in particular, the

number of users served by the bus-bar of the primary substation, divided by line and by voltage level.

**Table 13** Characteristics of users served by the primary substation

| *MV lines* | *N. MV/LV substations* | *N. MV/LV Transf.* | *Pn MV/LV Transf. (KVA)* | *N. LV users* | *N. MV users* |
|---|---|---|---|---|---|
| Sessano | 33 | 28 | 4,040 | 721 | 5 |
| Pesche | 45 | 38 | 5,090 | 1,651 | 9 |
| Carpinone | 9 | 8 | 2,016 | 1,493 | 1 |
| Colle Breccione | 23 | 15 | 1,740 | 685 | 11 |
| Polverone | 78 | 72 | 8,040 | 3,549 | 8 |
| Total | 192 | 165 | 20,840 | 8,099 | 34 |

There are 8.099 users. The total nominal power of active users, installed downstream TR1 transformer is 15,613 (kW) of which, 14,059 (kW) are in MV.

The nominal power ($P_d$) and agricultural or industrial sector of MV passive users are shown in Table 14.

**Table 14** MV passive users

| *MV lines* | *Pd (kW)* | *Agr. (%)* | *Ind. (%)* |
|---|---|---|---|
| Pesche | 3,531 | 30 | 70 |
| Sessano | 1,256 | 30 | 70 |
| Colle Breccione | 8,566 | 30 | 70 |
| Polverone | 2,323 | 30 | 70 |
| Carpinone | 562 | 30 | 70 |

The installed active power is constituted by hydroelectric plants, by photovoltaic systems, gas co-generators and turbo-gas, see Table 15.

**Table 15** MV/LV active users

| *MV lines* | *Photov. Pd (kW)* | *Hydroel. Pd (kW)* | *Co-gen. Pd (kW)* | *Turbo-gas Pd (kW)* |
|---|---|---|---|---|
| Pesche | 2,573 | 0 | 800 | 771 |
| Sessano | 0 | 2,800 | 0 | 0 |
| Colle Breccione | 0 | 5,030 | 302 | 0 |
| Polverone | 2,423 | 1,137 | 75 | 0 |
| Carpinone | 0 | 50 | 0 | 0 |

Two hydropower plants are currently installed downstream transformer TR1 of the primary substation: respectively of 3,300 (kW) and of 1,730 (kW) on one MV line (Colle Breccione); two hydro-plants, of 1,400 (kW) each one, are located on another MV line (Sessano); and finally, a plant of 1,137 (kW) is installed on another MV line (Polverone). Regarding MV line (Pesche), nine MV users are connected to it, 4 being active. Particularly in Pesche, the generation of MV/LV active users produces 4,144 (kW), of which 2,573 (kW) derived from photovoltaic sources, 771 (kW) from thermal source and the remaining 800 (kW) from other sources, are totally absent from the hydroelectric and wind power.

Producers in MV Pesche line are located mainly downstream of the line, in particular, we find a biogas plant and two photovoltaic plants respectively of 82 (kW) and 900 (kW). Near the primary substation, we find a photovoltaic plant of 1,000 (kW).

## 6.2 Simulink model

For the realisation of the Simulink model of the actual smart grid, SimPowerSystems libraries, which contain main components of an electric network and electrical specific systems, including the ones from renewable sources, have been used.

A model structure, with different layers, has been implemented. The highest hierarchical layer, constituted by functional blocks of the electrical components of Figure 10, is shown in Figure 11.

Referring to Figure 11, from left to right, the following blocks are distinguished: HV network, HV busbar, TR1, and Petersen coil resistance, stall processing and power factor correction are distinguished. In grey, the specific sub-networks of Pesche, Sessano, Colle Breccione, Polverone and Carpinone are represented. At the bottom left, there is the PowerGUI block and, at the top, a sub-system to compute transformer indexes (in orange) is present. HV network block represents the national transmission network at 150 kV by means of the component three-phase source: an ideal three phase voltage generator and internal impedance RL series. The internal resistance and inductance can be specified by directly entering the values of R (Ω) and L (H), or indirectly by specifying the power of short circuit in (VA) and the ratio X/R in (pu). In our model, the three-phase source is set as in Table 16.

**Table 16** Three-phase source parameters

| *Nominal voltage* | *Short circuit power* | *X/R* |
|---|---|---|
| 150 kV | 2,228 MVA | 7 |

HV bus-bar and the stall transformation blocks, in green, are blocks for the measurement of electrical parameters, such as line voltage, phase-to-ground, phase current, active and reactive power flow. These measures are exported by using MATLAB Workspace. TR1 block represents TR1 transformer of the primary substation of Carpinone and it is modelled using the component three-phase transformer (two windings). Such a block accurately simulates the actual transformer, allowing to set its primary and secondary windings type, its rated apparent power, the resistance and inductance of its two windings, its magnetic resistance and inductance. TR1 block is also able to model the saturation of the magnetic core.

**Figure 11** Simulink model of Carpinone grid (see online version for colours)

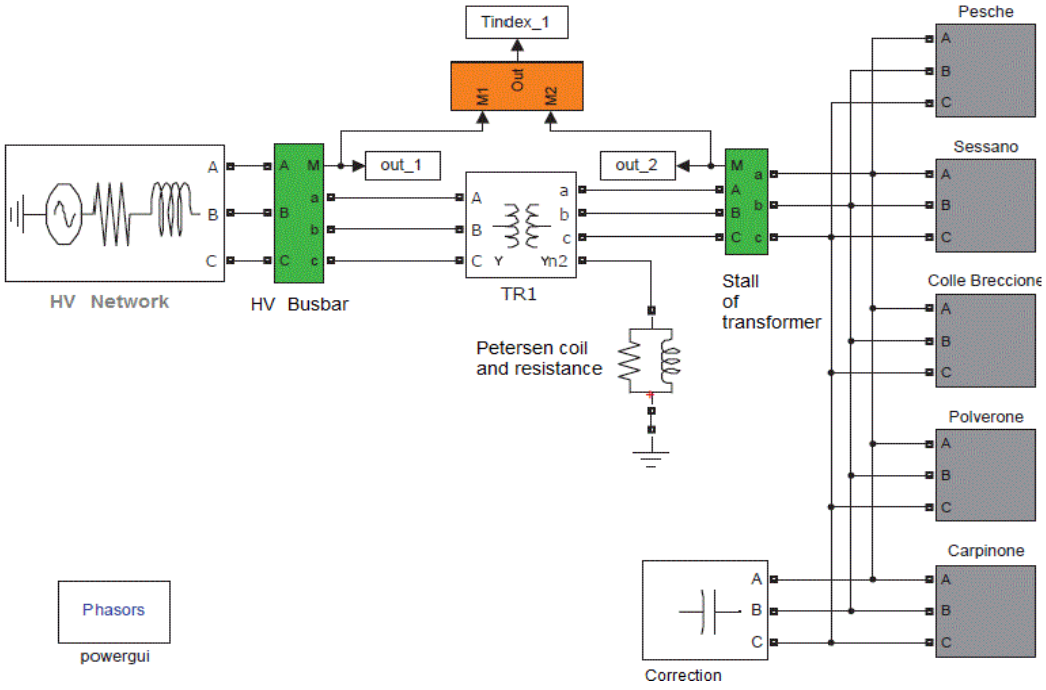


**Figure 12** Measure concentrated users block (see online version for colours)

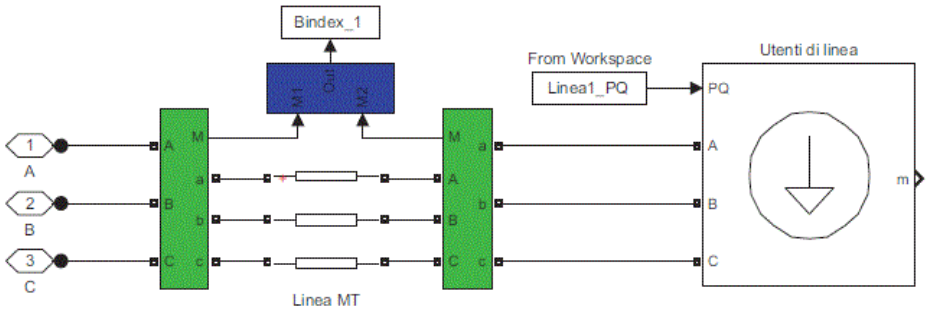


Petersen coil and resistance block model the impedance compensation of the neutral of the primary substation by means of a parallel RLC branch. The model considers the power factor correction capacitors of the primary substation of Carpinone by means of the three-phase series RLC load component, initialised to the value of 2.7 Mvar. Power GUI block is necessary for the simulation of any Simulink library components and it is used to store the equivalent circuit representing the model space state equations.

Computation of the load flow is based on Newton-Raphson method.

### *6.3 Computation results*

A series of simulations have been performed on the actual smart grid model, considering first just its passive users and then active and passive users as they are currently present in the MV/LV grid, to determine whether, in a given smart grid, the installed distributed generation (DG) implies or not benefits for the whole grid, compared to the situation of a purely passive grid.

Simulations have been performed considering Pesche, Sessano, Colle Breccione, Polverone and Carpinone as users concentrated in the 'centre of gravity' of the respective line MV. Figure 12 shows the measurement blocks (green colour), the sub-system for the calculation of the indexes of branch (blue colour), MT line blocks and members of the line, which respectively represent truncated MV lines and the set of MV/LV utilities of a given line.

The analysis of the results, depicted in Figures 13 and 14, shows that the presence of DG in the network implies enormous benefits in terms of the reduction of the power required from HV network, and of joule losses in the transformer of the primary substation.

Figures 15 and 16 respectively show the power and joule losses on Carpinone MV lines, in the case of passive and active networks.

**Figure 13** Power required from HV network (see online version for colours)

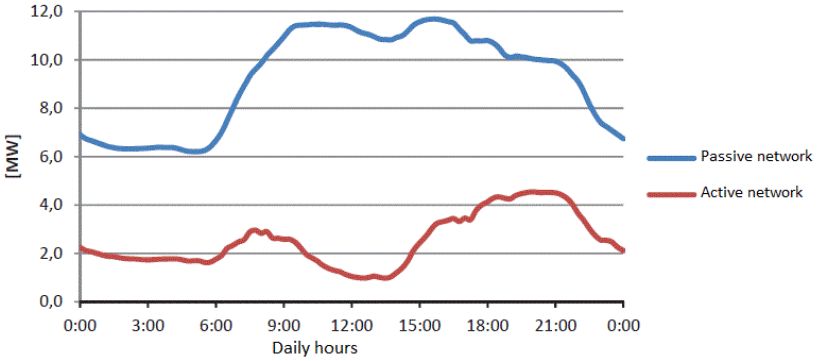


**Figure 14** Joule losses in the transformer (see online version for colours)

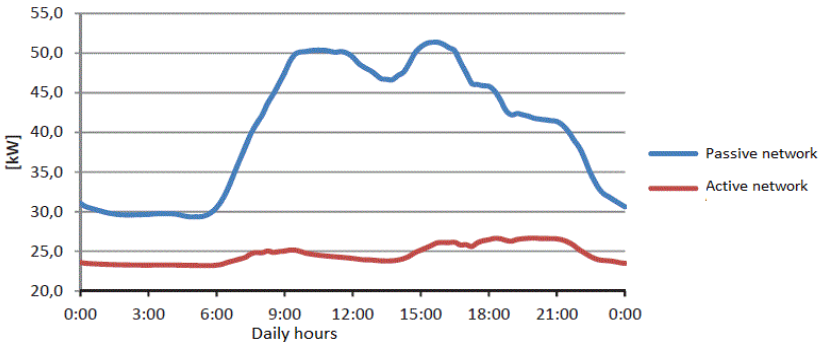


**Figure 15** Power on Carpinone MV lines (see online version for colours)

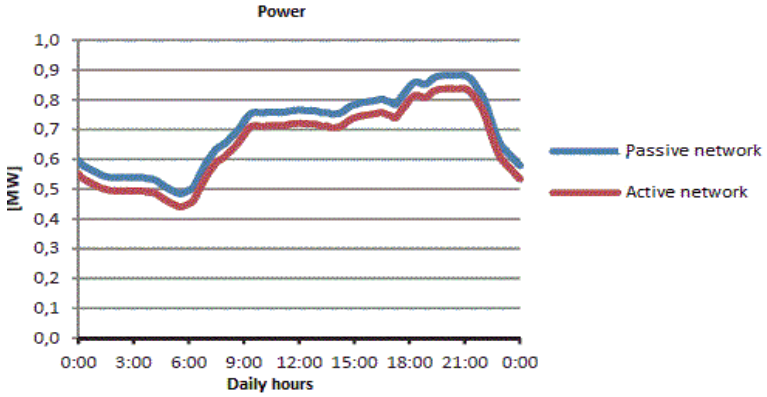


**Figure 16** Joule losses on Carpinone MV lines (see online version for colours)

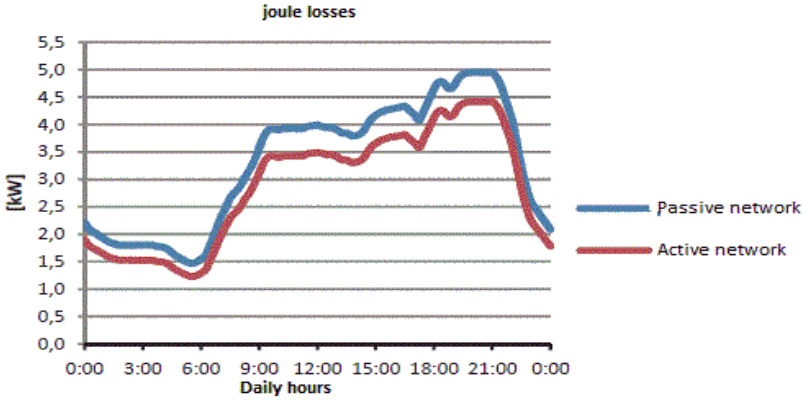

The values of indicators, reported in Figures 13, 14, 15 and 16 show an improvement of energy efficiency, owing to distributed generations, at the level of primary substation and MV lines. Such an improvement could be completely lost if the power due to the distributed generation is greater than the power needed to the passive users of the MV lines. In such a case an inversion of power flow in the primary substation and an increasing of joule losses could occur.

Further, we also analysed energy efficiency indicators in case of installation of new photovoltaic plants, of different sizes and locations, at Carpinone MV line of the Carpinone smart grid. Simulations have been performed, by adding one PV plant of a specific power in a different location for each simulation, on the electrical scheme of the Caripinone line of Figure 17(a), with the passive users of Table 14 and represented by the Simulink model of Figure 17(b).

As an example, a comparison of power at the bus-bar of Carpinone MV line in case of actual users (blue) and in case of adding a photovoltaic plant (green) of 1 MV, first connected upstream, between the substation CS UT MT and substation CS ENEL 1 and then connected downstream the substation CS ENEL 8 by a 0.5 (km) trunk, has been performed. In Figure 18, an inversion of power towards the primary substation occurs for five hours and 45 minutes.

**Figure 17** (a) The electrical scheme of Carpinone MV line and (b) its Simulink model (see online version for colours)

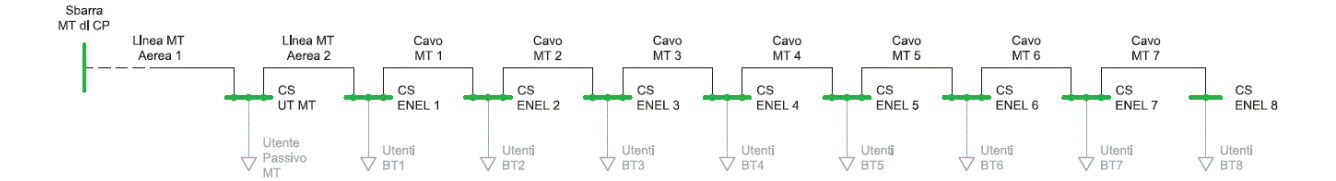


(a)

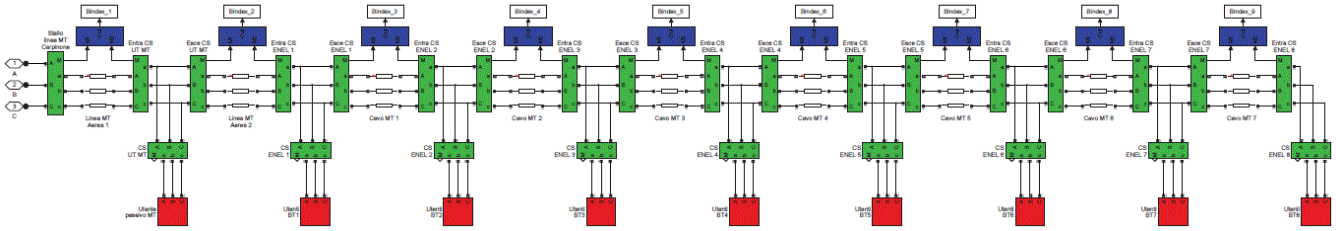

(b)

**Figure 18** Power comparison at the bus-bar of Carpinone MV line (see online version for colours)

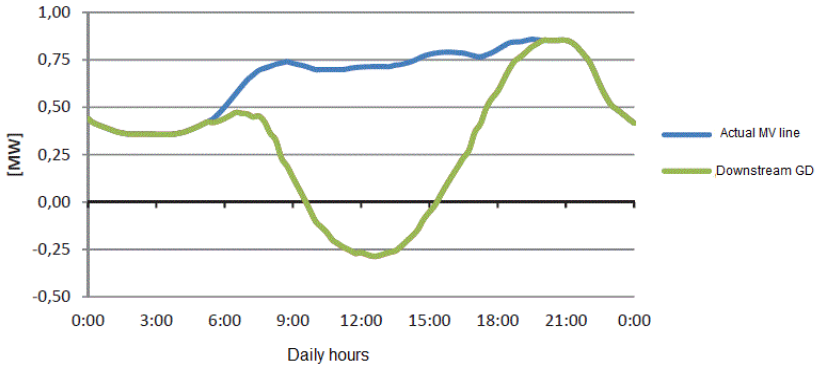


**Figure 19** Comparison of joule losses on MV line (see online version for colours)

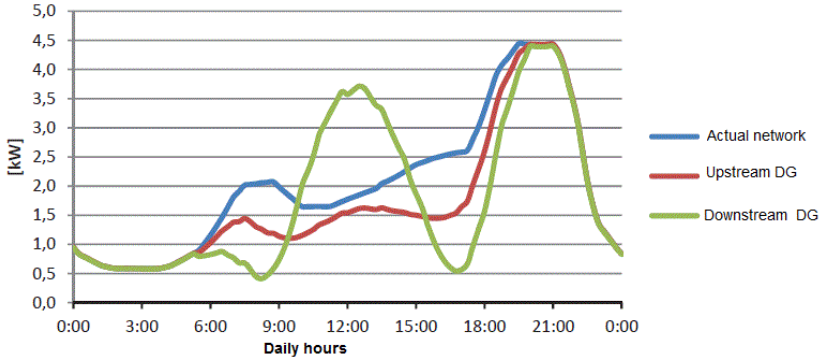

In Figure 19, the total joule losses on the same MV line are shown.

The presence of the downstream DG implies an increment of line losses owing to the presence of the upstream DG. Such an increment is more evident between 9:30 and 15:30, when the DG due to the photovoltaic plant reaches its maximum daily production.

## 7 Conclusions and future work

We are investigating integrated models to compute energy efficiency of interdependent urban networks in planning and operation scenarios. Models are under development in incremental fashion. In a first step, models of each basic network have been built to select adequate simulation platforms and to identify main parameters, characteristics and performance indicators of each network. In the second step, we built the model of the actual smart grid of Carpinone, operated by ENEL Distribuzione. A sensitivity analysis, conducted by means of series of simulations, has been performed, to evaluate whether, in the given smart grid, the installed distributed generation (DG), and its variability in location and in power, implies or not benefits on the efficiency of the whole distribution grid. The sensitivity analysis shows that the increment of DG in the grid may imply benefits of energy efficiency, in terms of reduction of the power required from HV network, and of joule losses in the transformer of the primary substation. The value of such benefits depends upon the power and location of the DG. Energy efficiency benefits are completely lost when the DG power is greater than the power needed by the passive users of the MV lines. In such a case, an inversion of power flow in the primary substation and an increment of joule losses will occur. The paper also presents different conceptual elements to extend the sensitivity analysis on to other local energy vectors (hydroelectric and gas powered electrical plants) and different storage solutions. For such a scope, an integrated model of smart grid, gas and water network is under development.

The scalability of the described models, in planning and operation scenarios of the city of Catania, Italy, is a very important step. The role of electricity, gas and water utilities, as stakeholders of SINERGREEN project, becomes more and more relevant in extending and tuning scenarios and models according to their actual needs.

## References

Abate, V., Adacher, L. and Pascucci, F. (2014) 'Situation awareness in critical infrastructures', *International Journal of Simulation and Process Modelling (IJSPM)*, Vol. 9, Nos. 1/2, DOI 10.1504/IJSPM.2014.061451.

Ahmad, N., Ghani, N.A., Kamil, A.A. and Tahar, R.M. (2015) 'Modelling the complexity of emergency department operations using hybrid simulation', *International Journal of Simulation and Process Modelling (IJSPM)*, Vol. 10, No. 4, DOI: 10.1504/IJSPM.2015.072537.

Alonge, G., Ciancamerla, E., Fallone, M., Mastrilli, A., Minichino, M., Ranno, M., Reali, M. and Regina, P. (2014) 'Modelling interdependent urban networks in planning and operation scenarios', *DHSS 2014 International Defense and Homeland Security Simulation Workshop*, 10–12 September, Bordeaux, France.

Bobbio, A., Bonanni, G., Ciancamerla, E., Clemente, R., Iacomini, A., Minichino, M., Scarlatti, A., Terruggia, R. and Zendri, E. (2010) 'Unavailability of critical SCADA communication links interconnecting a power grid and a telco network', *Reliability Engineering and System Safety Journal*, Vol. 95, No. 12, pp.1345–1357.

Bruzzone, A.G., Massei, M. and Poggi, S. (2016) 'Infrastructures protection based on heterogeneous networks', *International Journal of Simulation and Process Modelling (IJSPM)*, Vol. 11, No. 1, DOI: 10.1504/IJSPM.2016.075078.

Ciancamerla, E., Lefevre, D. and Minichino, M. (2011) 'Service dependability and performance of SCADA systems interconnecting power grids and telco networks', *Annual Conference of the European Safety and Reliability Association*, Troyes, France, ISBN 978-0-203-13510-5 (eBook).

Enel (2013) *Enel Distribuzione S.p.A*., *Progetto Isernia: V Relazione semestrale di avanzamento*, Settembre.

Gil-Garcia, J.R., Pardo, T.A. and Nam, T. (2016) *Smarter as the New Urban Agenda – A Comprehensive View of the 21st Century City*, Public Administration and Information Technology, Vol. 11, ISBN:978-3-319-17619-2, Springer.

Hutterer, S. and Affenzeller, M. (2015) 'Dynamic optimal power flow control with simulation-based evolutionary policy-function approximation', *International Journal of Simulation and Process Modelling (IJSPM)*, Vol. 10, No. 3, DOI: 10.1504/IJSPM.2015.071379.

Mets, K., Ojea, J.A. and Develder, C. (2014) 'Combining power and communication network simulation for cost-effective smart grid analysis', *IEEE Commun. Surveys & Tutorials – Special Issue on Energy and Smart Grid.*

Shafiullah, G.M., Oo, A.M.T., Ali, A.B.M.S. and Wolfs, P. (2013) 'Smart grid for a sustainable future', *Smart Grid and Renewable Energy*, Vol. 4, No. 1, pp.23–34, DOI:10.4236/sgre.2013.